Estimating the Bohr Magneton Through Investigation of the Zeeman Effect in Cadmium Energy Levels

Lab 3 – PHYS2060

Henry Pickersgill – 201004137

Calculating μ_B using the Zeeman Effect

Abstract:

The Bohr Magneton is estimated through considering the Zeeman effect. Two experimental designs were used – one to study interference patterns using an eyepiece and the other using a CCD camera. The results found for the eyepiece experiment ($(9.4 \pm 2) \times 10^{-24} JT^{-1}$) agreed with the accepted value for the Bohr magneton ($9.24 \times 10^{-24} JT^{-1}$). The results found for the CCD experiment varied greatly, with an average of $(11.6 \pm 2) \times 10^{-24} JT^{-1}$.

Introduction:

The *Zeeman Effect* describes the process of splitting of spectral lines (fine-structure splitting [1]), named after Pieter Zeeman, and can be investigated through observation of interference patterns. Through this, we can identify the energy levels of atoms and quantify them with respect to the angular momentum of an electron [2].

The *Bohr Magneton*, μ_B, *is* a quantity that expresses the magnetic moment of an electron due to either spin or orbital angular momentum. This quantity is defined by equation (1):

$$\mu_B = \frac{he}{4\pi \cdot m_e} \quad (1)$$

Where $h = 6.626 \times 10^{-34} Js$, $e = 1.6 \times 10^{-19} C$ and $m_e = 9.11 \times 10^{-31} Kg$ [3].

The *anomalous* Zeeman effect considers the splitting of a spectral line into multiple fine structure lines due to an applied magnetic field, B. Depending on the electron's orbital angular momentum, L, the spectral lines split into a total of $2L + 1$ finer lines [1][4]. Spectral lines correspond to one specific energy and hence the energy levels contained within an atom are *quantised*; the effect of the magnetic field is to produce finer energy levels, which have been shifted an amount ΔE from the original levels. This shift energy can be quantified in terms of μ_B and the strength of the applied magnetic field:

$$\Delta E = B \cdot \mu_B \quad (2)$$

Therefore, if we can study the fringes in an interference pattern, we can estimate the energy shift ΔE and hence the μ_B if the strength of the magnetic field is known.

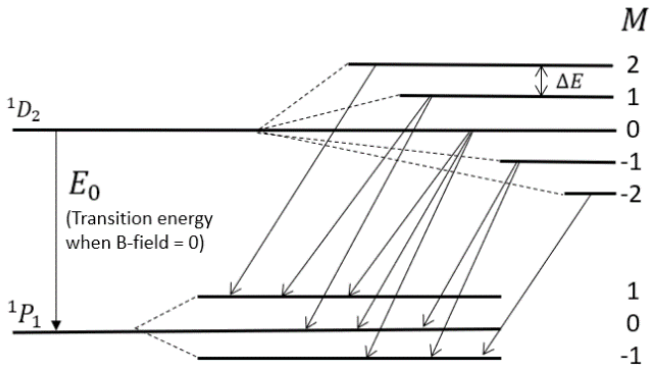

Figure 1: *The various possible energy level transitions for electrons within Cadmium, where M is the magnetic quantum number. For when B = 0 and B ≠ 0.*

Figure 1 demonstrates the effect of an applied magnetic field on the spectral line energy levels; the energy gap between split levels, ΔE, remains constant throughout. There exist three possible transitional energies, corresponding to the transitions from $\sigma^{\pm}$ and π Zeeman components. These energy transitions are dependent on the change in *magnetic angular momentum* quantum number, ΔM_J, which can either be ± 1 or 0 [5]. The $\sigma^{\pm}$ Zeeman components correspond to transitions with change $\Delta M_J = \pm 1$, and the π components correspond to transitions involving no change in M_J [4].

To estimate the Bohr magneton, a lamp can be placed within a magnetic field to produce the Zeeman pattern. Lenses may be used to focus the

light onto a *Fabry-Perot Etalon*, which is a high-resolution spectrometer consisting of two parallel, semi-reflective surfaces. This spectrometer can be used to detect extremely fine shifts in wavelength and hence energy [6].

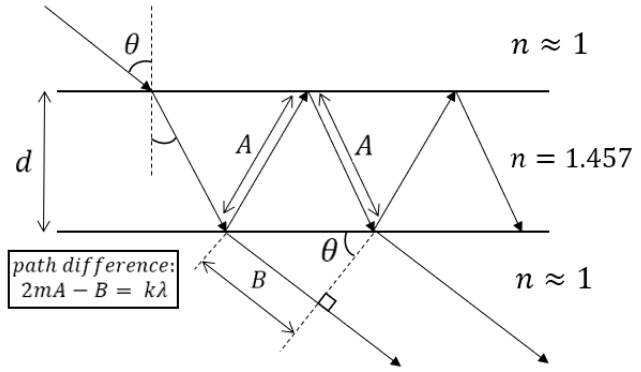

Figure 2: *A schematic diagram of the function of the Fabry-Perot Etalon.*

Figure 2 represents the typical function of a Fabry-Perot Etalon. The reflected light ray travels an extra distance $2mA$, where m is an integer. The materials do not internally reflect light rays perfectly however, as some of the light is refracted during each boundary collision, causing interference with other photons [2]. We can the *etalon equation* due to interference between the reflected and refracted rays as depicted in *figure 2*:

$$x_{diff} = 2d\sqrt{n^2 - sin^2\theta} = k\lambda \qquad (3)$$

where d is the separation of the two reflective surfaces, n is the refractive index within the etalon (known to be $n = 1.457$), θ is the incident angle and $k\lambda$ is an integer multiple of the wavelength of the incident light [1]. *Figure 3* portrays a typical interference pattern produced after the incident light is passed through two lenses, the etalon, and a colour filter. The splitting due to an applied magnetic field can be observed. This pattern can be studied using an eyepiece or recorded using software receiving data from a CCD (charge-coupled device) camera.

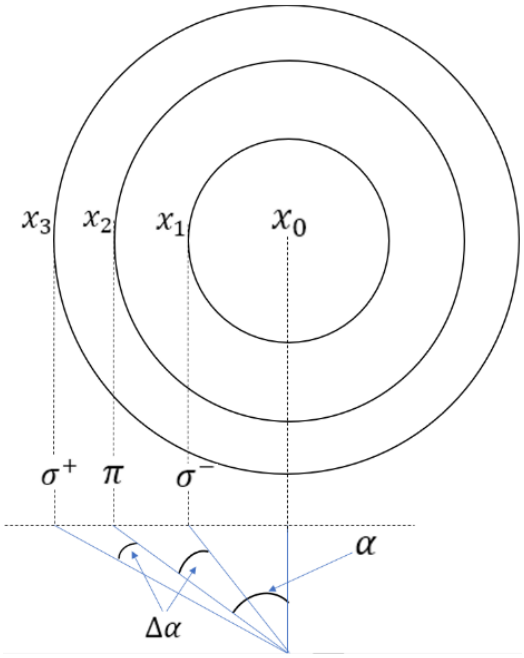

Figure 3: *The central Zeeman triplet within the interference pattern, observed using an eyepiece.*

The angle between the centre of the pattern and the rings can be calculated using simple trigonometry:

$$\alpha_n \approx \tan(\alpha_n) = \frac{|x_0 - x_n|}{\text{focal length}} \qquad (4)$$

Where α_n is the angle from the centre of the pattern to the n^{th} position, x_n. Small angles are assumed, and we can arrive at an expression for the energy shift in terms of α, and the difference between this angle and either of the σ components (shift angle), $\Delta\alpha$:

$$\Delta E \approx \frac{-\alpha\Delta\alpha \cdot E_\gamma}{n^2} \qquad (5)$$

E_γ represents the energy of the photon incident into the Fabry-Perot etalon, where

$$E_\gamma = \frac{hc}{\lambda} \qquad (6)$$

The quantity λ in equation (6) references the wavelength of the emitted Cd light: $\lambda = 643.847\ \text{nm}$ [4]. Furthermore, this allows the derivation of the formula for the Bohr magneton:

$$\mu_B = \frac{\Delta E}{B} \approx \frac{-\alpha\Delta\alpha \cdot hc}{B\lambda n^2} \qquad (7)$$

In the Zeeman interference pattern, the positions and the angles of the specific rings can be recorded. Using equation (7), the Bohr Magneton can be estimated. A range of values for the shift energy, ΔE, can be recorded for a variety of magnetic field strengths, B. Equation (7) suggests a linear relationship between ΔE and B with a gradient equal to μ_B.

Method I:

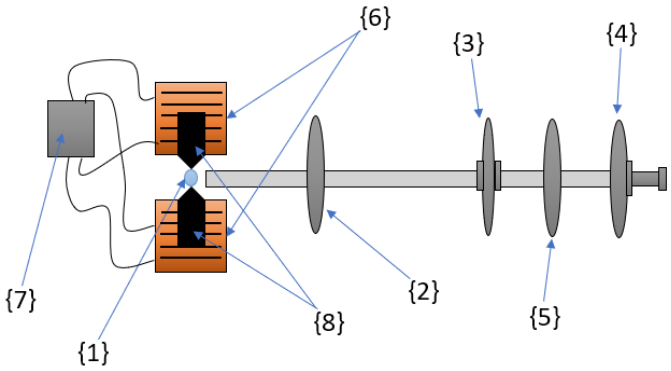

Figure 4.1: *A schematic diagram presenting a birds-eye view of the setup and function of the experiment.*

The experimental setup is shown in *figure 4.1* above. Importantly, the setup is arranged in a transverse configuration as depicted in *figure 4.2*.

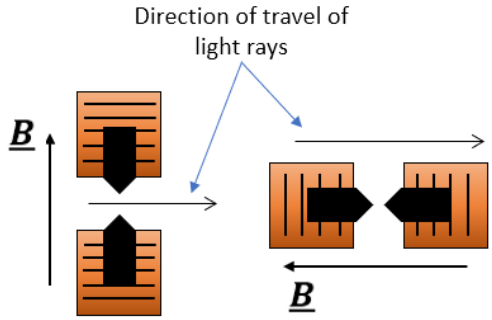

Figure 4.2: *A demonstration of the possible configurations of the experimental apparatus: transverse (left) and longitudinal (right).*

Light rays are focused onto the Cd lamp {1} through a condenser lens {2} which optimises the brightness of the light. Next, the light passes through the Fabry-Perot spectrometer {3}, which creates the concentric ring interference pattern which will be studied using the eyepiece, which contains a colour filter {4}. The final lens, the imaging lens {5}, ensures that the interference pattern is within focus and the rings are very clearly resolved. Two coils of wire surround the Cd lamp, creating a uniform magnetic field between the coils when a current is supplied. These coils {6} are connected to a power supply {7} in series to ensure that the induced magnetic fields point in the **same** direction; otherwise they would cancel, proven using the right-hand rule [4]. This induced magnetic field passes through two pole pieces {8}, which ensure the magnetic field is uniformly focused onto the Cd lamp. These pieces are securely clamped down to avoid shattering the Cd lamp when a magnetic field is applied.

For the purposes of this experiment, the central fringe triplet was chosen (as is shown in *figure 3*), as it was easiest to determine the positions of the rings this way. A reference point was used throughout the calculations, x_0. The entire eyepiece component could be adjusted laterally, to centre the internal crosshairs onto a single ring of the triplet. The positions $x_{1,2,3,4,5,6}$ were measured and so the angles $\alpha_{1,2,3,4,5,6}$ were calculated using equation (4) – this was achieved due to the symmetrical nature of the pattern. The *focal length* of the imaging lens was stated as 150mm [4], although it was decided to assume some uncertainty in this quantity, hence $f = (150 \pm 5)\text{mm}$.

As is evident from *figure 3*, the shift angle, $\Delta\alpha$ is equal to the difference between the angle to the π Zeeman component and the adjacent σ components. Hence, due to the symmetry of the pattern, four values for $\Delta\alpha$ were evaluated and two values for α were known (α_2 and α_5). Hence, four values for the Bohr magneton could be estimated using equation (7).

To achieve this, all the quantities within the equation were known besides the magnetic field strength, B. The current at which the Zeeman interference pattern was observed was recorded as $I = (6.1 \pm 0.01)A$; once the lamp was suitably cool to remove, the magnetic field strength was measured using a Teslameter. The magnetic field strength was measured as $B = (392 \pm 10)mT$, with the error estimate determined from the fluctuating readings.

The uncertainties in each calculated value were determined from the quantities $\alpha, \Delta\alpha$ and B. For the purposes of this experiment, the quantity $\frac{hc}{\lambda n^2}$ was assumed to have no uncertainty.

Method II:

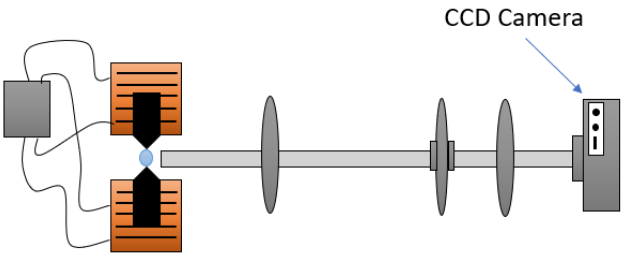

Figure 5: *A schematic diagram presenting a birds-eye view of the setup of the experiment. A CCD camera replaces the eyepiece.*

The setup for the second part of this experiment is shown in *figure 5* above. For this part, the eyepiece is replaced with a CCD camera containing a one-dimensional array of pixels. The pattern cannot be observed manually when the CCD camera is placed in the setup. Therefore, the etalon and lenses needed to be adjusted while observing the pattern through the eyepiece. When the arrangement was in its optimal configuration, a clear interference pattern was seen using computer software.

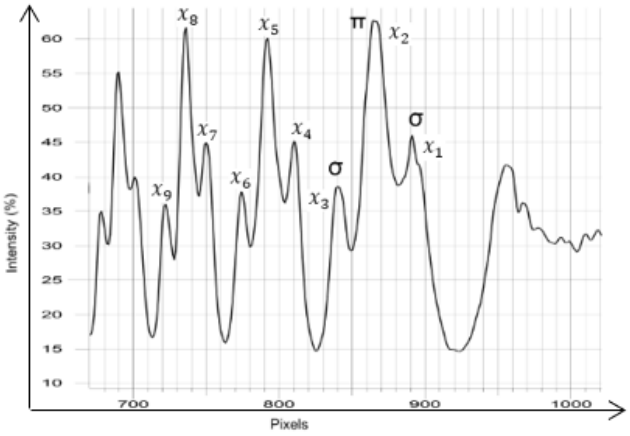

Figure 6: *The visible interference pattern produced by "slicing" the typical ring pattern horizontally [7].*

Figure 6 displays the typical pattern produced by the CCD camera with non-zero magnetic field, representing a "slice" of the 2-D ring pattern [7]. However, only the left side of the pattern was included in the data as it became difficult to resolve both sides of the pattern simultaneously. Three separate Zeeman triplets were used in this section. The peaks labelled with positions $x_{1,2,\ldots,9}$ correspond to the separate rings in each Zeeman triplet. These positions could be recorded in terms of pixels and converted into distances, where each pixel is $14\mu m$ wide [4]. An appropriate error for each position reading was estimated: $\pm 5 \text{ pixels} = \pm 70\mu m$.

As in Method I, the angles $\alpha_{1,2,\ldots,9}$ were evaluated using equation (4). The shift angles, $\Delta\alpha$, were determined as the difference between the angles to each of the π peaks ($\alpha_2, \alpha_5, \alpha_8$) and the adjacent σ peaks. The shift energies, ΔE, were evaluated using equation (5) and (6). The procedure was repeated for six more magnetic field strengths, and hence three graphs of ΔE against B were constructed (one for each Zeeman triplet). As is predicted by equation (7), the gradient of each of these graphs provides an estimate for the Bohr magneton, μ_B.

Results:

The determined values for μ_B, using the eyepiece, are shown in *table 1 below*.

Angles used	Bohr magneton, μ_B $(10^{-24} JT^{-1})$
α_2 and $\Delta\alpha$ $^{(1)}$	$-(6.6 \pm 0.8)$
α_5 and $\Delta\alpha$ $^{(1)}$	$-(5.9 \pm 0.8)$
α_2 and $\Delta\alpha$ $^{(2)}$	$-(13.2 \pm 2)$
α_5 and $\Delta\alpha$ $^{(2)}$	$-(11.9 \pm 2)$

Table 1: *Estimates for the Bohr magneton using equation (7), for the various combinations of the angle α and the shift angle $\Delta\alpha$.*

This corresponds to an average value, $\mu_B = (9.4 \pm 2) \times 10^{-24} JT^{-1}$. The individual results show significant fluctuation.

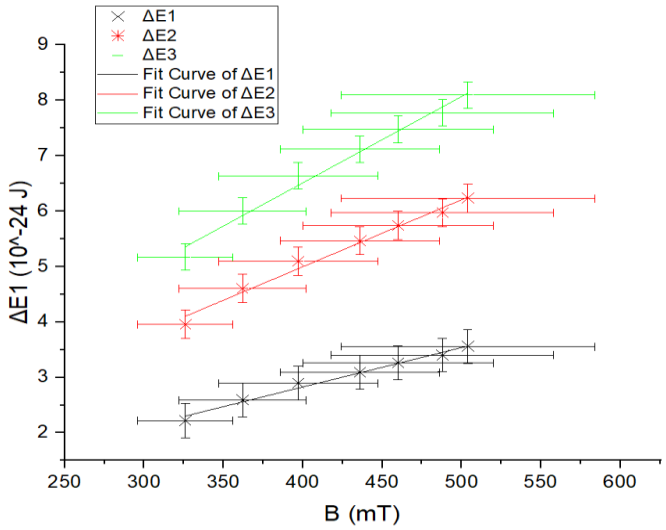

Figure 7: *Three graphs of the energy shift against the applied magnetic field, with linear fits appropriately estimated.*

Figure 7 demonstrates the linear relationship between the energy shift, ΔE and the magnetic field strength, B. This is evident by the R^2 values for each of the graphs (0.98618, 0.98591 and 0.98617 for the inner, centre and outer Zeeman triplets respectively). The gradients, the Bohr magneton estimates, of each of these graphs are displayed in *table 2* below.

Zeeman Triplet	Bohr magneton estimates, μ_B $(10^{-24}JT^{-1})$
Inner triplet (x_1, x_2, x_3)	$-(7.1 \pm 0.4)$
Centre triplet (x_4, x_5, x_6)	$-(12.1 \pm 0.6)$
Outer triplet (x_7, x_8, x_9)	$-(15.6 \pm 0.8)$

Table 2: *Calculated gradients for the graphs of energy shift against magnetic field strength, for each of the three Zeeman triplets investigated.*

This corresponds to an average value $\mu_B = (11.6 \pm 2) \times 10^{-24}JT^{-1}$. Once again, the estimates differ significantly.

Discussion:

Table 1 suggests that there were certainly very significant errors in some of the readings. The estimates for the Bohr magneton vary greatly, and the uncertainties in each individual measurement are significant. An average value was calculated, however, due to the large discrepancy between the four estimates, this average can be considered inappropriate. With reference to *figure 7*, we can clearly see strong linear relationships between the energy gap between Zeeman component energy levels, ΔE and the varying magnetic field strength, B. This is as was predicted earlier, and therefore the theory can be proven to hold. Nevertheless, the error bars are very large for the magnetic field measurement. This was discussed earlier, these estimates for the uncertainty in B were chosen as appropriate. This was due to the extreme variation in the Teslameter readings due to minute changes in the position of the probe. *Table 2*, again, shows large variations in the estimates for μ_B within a similar range to that in *table 1*. An average was also calculated for these three estimates. The accepted value for the Bohr magneton is [1]:

$$\mu_B = 5.79 \times 10^{-5}\text{eVT}^{-1} = 9.24 \times 10^{-24}\text{JT}^{-1}$$

We can see from *table 2* that the estimate increases as we increase the distance from the centre of the interference pattern. This may be due to a source of error – the interference pattern becomes noticeably condensed the further from the centre we observe.

Conclusion:

The study of this experiment was the *Zeeman Effect* and the physical unit of magnetism; the *Bohr Magneton, μ_B*. Using lenses and a *Fabry-Perot spectrometer*, an interference pattern of Cadmium light was created. These patterns manifest as concentric rings, where each ring represents a different energy level within the atom. The Zeeman effect allowed the study of fine-structure splitting; the separation of singular energy levels due to the action of an external magnetic field on electron spin. The aim of this experiment was to produce some estimates for the value of μ_B, by investigating the

interference patterns using an eyepiece and CCD camera. The positions and angles to the split peaks were measured using the eyepiece, and estimates averaged $\mu_B = (9.4 \pm 2) \times 10^{-24}\text{JT}^{-1}$. The accepted value for this quantity is $\mu_B = 9.24 \times 10^{-24}\text{JT}^{-1}$. This corresponds to a 1.7% difference. Therefore, it can be concluded that these estimates agree with the known value for μ_B. The positions and angles of nine peaks were recorded using software and a CCD camera and allowed the generation of four more estimates for μ_B. The average of these four estimates was $\mu_B = (11.6 \pm 2) \times 10^{-24}JT^{-1}$. This average is within approximately 23% of the accepted value for μ_B, suggesting there were clear problems with the experimental method.

All the estimates for μ_B had considerable uncertainties, and this is likely due in part to the dramatic uncertainty in the measurement of the magnetic field strength. A potential source of error for this experiment may be the difficulty in arranging each part of the apparatus perfectly. The lenses, lamp and etalon were required to be perpendicular to the path of light and perfectly arranged in height and distance from the lamp. Any deviance from this setup could have caused some shift in the interference pattern and hence inaccurate readings of position – therefore, inaccurate measurements in the angles.

The average value of the eyepiece experiment was well within the range of the accepted value for μ_B, while the average value for the CCD experiment deviated significantly. This may be since for the first part of the experiment, only the central Zeeman triplet was used. In the second part, three separate Zeeman triplets were used. The value for μ_B seemed to increase with increasing distance from the centre of the pattern. The fringes in the pattern were, in fact, **not** equally spaced as they appeared to converge when observing further out from the centre. Equation (7) relies on the approximation:

$$tan\theta \approx \theta \text{ , for small } \theta$$

Therefore, the further out we observe, the larger the angle, and hence the more inaccurate this approximation becomes. This may be a source of the increasing error in μ_B for the outer Zeeman triplets.

One potential improvement for this experiment would be to spend significantly longer ensuring that the apparatus is optimally configured. The pattern observed by the CCD was severely biased to the left-hand side as it required extreme precision to produce the desired symmetrical interference pattern. This may have skewed the results. It may be beneficial to repeat the experiment in different situations, such as decreased ambient lighting, to reduce the noise present in the interference pattern. Also, it would be useful to repeat the procedures with lamps of different elements, such as Sodium or Mercury, to possibly prove or disprove the validity of the experiment.

References:

[1] Tipler P. A., Mosca G. (2007). *Physics for Scientists and Engineers (with Modern Physics) 6th Edition.* W H. Freeman. pp.1242-1246.

[2] Boudet R. (2009). *Relativistic Transitions in the Hydrogenic Atoms*. Berlin: Springer-Verlag. pp.95-96.

[3] Liebes S. Jr., Franken P. (1959). Magnetic Moment of the Proton in Units of the Bohr Magneton; the Magnetic Moment of the Electron. *Physical Review,* 116(**3**), pp.633-650.

[4] Leeds University School of Physics and Astronomy. (2018-2019). *PHYS 2060 and PHYS2110 Guidance and Scripts Handbook.* pp.107-126

[5] Richtmyer F K., Kennard E H., Cooper J N. (1969). *Introduction to Modern Physics, 6th Edition.* McGraw-Hill.

[6] Ismail N., Kores C., Geskus D., Pollnau M. (2016). Fabry-Pérot resonator: spectral line shapes, generic and related Airy distributions, linewidths, finesses, and performance at low or frequency-dependent reflectivity. *Optics Express*, 24(**15**), p.16366.

[7] Welch R. (2016). *Calculation of the Bohr Magneton Using the Zeeman Effect*. [Online]. Available from: *https://robwel.ch/2014/05/calculation-of-the-bohr-magneton-using-the-zeeman-effect/.* [Accessed 06/12/2018]